UC Davis
Civil & Environmental Engineering

Title
Parametric Study of Liquefaction Induced Downdrag on Axially Loaded Piles

Permalink
https://escholarship.org/uc/item/06b3p6g4

ISBN
9780429031274

Authors
Sinha, Sumeet Kumar
Ziotopoulou, Katerina
Kutter, Bruce L

Publication Date
2019-06-01

DOI
10.1201/9780429031274

Data Availability
The data associated with this publication are available upon request.

Peer reviewed

eScholarship.org Powered by the California Digital Library
University of California

Parametric study of liquefaction induced downdrag on axially loaded piles

S.K. Sinha, K. Ziotopoulou & B.L. Kutter
University of California Davis, USA

ABSTRACT: Earthquake-induced liquefaction typically causes soil settlement which may lead to downdrag in axially loaded piles. The drag load generated may overstress the pile or cause significant foundation settlements. Despite significant research progress on the effects of liquefaction on structures and the seismic response of piles, there is still a knowledge gap in the assessment of liquefaction-induced downdrag. This paper discusses different factors that govern this mechanism and presents a parametric study performed using the AASHTO-recommended neutral plane method using displacement-based t-z spring analyses on a simplified profile where liquefiable layer depth and thickness, reconsolidation strains in dense and loose sand, tip conditions, and pile types (L/D ratios) are varied. The results obtained from this preliminary analysis draw some important conclusions regarding performance of large, medium, and slender piles and are used to design centrifuge model tests to further investigate and understand the complex mechanisms under more realistic conditions.

1 INTRODUCTION

Piles are one of the most common and efficient foundation types capable of transferring high structural loads through weak soil layers to more competent soils at greater depths. However, during strong seismic events, liquefaction and the associated excess pore-pressure generation in surrounding saturated soils can lead to loss of shear strength, settlement of soil, and lateral spreading depending on the boundary conditions. These conditions not only weaken the overall soil-pile stiffness but also impose additional vertical and lateral loads, which can lead to several possible modes of failure such as bearing failure, buckling and bending of the pile, and excessive settlement. Following liquefaction, excess pore pressures dissipate, soil grains sediment and the soil layer reconsolidates. For axially loaded piles, liquefaction-induced settlement shifts the neutral plane (i.e. location of zero relative soil-pile settlement) downwards, generates internal drag loads (i.e. integral of negative skin friction), and drags the pile downwards resulting in overall settlement of the pile which is termed as downdrag (i.e. the settlement of soil at the neutral plane) (see Fig 1.). This not only increases the load on the pile but also reduces the positive skin friction resistance, resulting in an overall increase of load and settlement at the pile tip and making downdrag both a load transfer as well as a settlement problem.

There are many factors that determine and influence the downdrag of axially loaded piles (Fig. 1). The soil profile itself can greatly influence the development of drag load and various researchers have investigated these effects. Boulanger & Brandenberg (2004) proposed a modified neutral plane method to analytically evaluate downdrag in piles. However, the proposed method was developed for a sand layer sandwiched between two clay layers, which is not widely applicable. Fellenius & Siegel (2008) showed that the presence of a liquefiable layer below the initial static neutral plane can result in large drag loads and is more detrimental than the one above it. A thicker liquefiable layer results in higher reconsolidation settlement and thus higher drag load. Another factor can be the pile diameter (L/D ratio) and tip condition. A floating tip can result in lower drag load but higher downdrag as compared to a tip resting on a rigid layer. Consequently, a pile with

a larger diameter will result in a smaller tip movement compared to one with a smaller diameter resulting in comparatively higher drag load and smaller downdrag.

The time-dependent phenomenon of excess pore pressure generation and dissipation affects both the shear strength of soil and the settlement experienced by the soil-pile system. Coelho et al. (2004) performed dynamic centrifuge model testing on uniform saturated deposits of relatively loose and dense sand and showed that the excess pore pressure and post-liquefaction reconsolidation develop not only in loose sands but also in densely saturated sands. Knappett & Madabhushi (2006) showed that as the excess pore pressure at the pile tip increases, the load carried by the tip reduces and settlement occurs. Another group of research efforts (Ashford et al. 2004; Rollins et al. 2005; Rollins & Hollenbaugh 2015; Rollins & Strand 2006) focused on blast-induced liquefaction tests and showed 80% of the settlements happen within the first 5-10 minutes after blasting even though it can take about an hour or more to achieve full reconsolidation. Reconsolidation strains in liquefied soils were measured to be around 2-3% but the relative evolution of all the phenomena was not tracked. Post-reconsolidation, the skin friction in the liquefied soil was measured around 50% of the positive skin friction and in the non-liquefied soils, it decreased by 10-20%. However, since these tests were not monitored for a long time, it can be expected that over time the skin friction in liquefied/non-liquefied soils might return to its full capacity. There are also other factors such as the pore-pressure generation/dissipation pattern and presence of any surface cracks and interface gaps (Fig. 1) that can affect the hydraulic boundary conditions, sequencing of settlement, and thus the overall development of the downdrag phenomenon.

While some of the above factors have been studied, others like the pore-pressure generation/ dissipation pattern, sequencing of settlements, surface cracks, interface gaps, presence of a clay layer above the liquefiable layer have not been fully investigated in the literature. Existing numerical methods lack in their capabilities to model these mechanisms while the absence of experimental data makes it challenging to hypothesize, develop, and validate new models. This warrants a well-instrumented and properly designed experiment can potentially capture these effects and assist their further study.

This paper presents the results of an initial simplified analysis performed to understand the downdrag phenomenon and then design the centrifuge model tests to fully investigate the complex mechanism. AASHTO (2014) and the sponsor Caltrans recommended neutral plane method with displacement based simplified t-z spring analysis is used to perform a parametric study of pile type (L/D ratio), tip condition, depth and thickness of the liquefiable layer, reconsolidation strains in the loose and dense soil, and pile head load. With the assumption of no compressible layers in the profile as well as no prior liquefaction events, the initial static neutral plane is considered at the surface. The post-liquefaction induced settlement (after full reconsolidation and dissipation of all excess pore-pressure) is used to define the soil settlement profile in the analysis.

It must be noted that the analysis presented herein does not consider and model the excess pore-pressure generation/dissipation and its effect on the soil-pile interface behavior. Despite the limitations in this simplified method, conclusions drawn in terms of downdrag, neutral plane location, and pile settlement for large, medium and slender piles still remain useful and are important to be noted. The results and understanding obtained through these analyses are ultimately used in deciding a model pile and soil profile for designing large centrifuge tests at the Center for Geotechnical Modeling (CGM) at the University of California, Davis. The experiments will help to study and understand the mechanisms that cannot be modeled by the existing numerical methods and most importantly provide quantitative results on the relationship between excess pore pressure dissipation, negative friction development and settlement.

2 T-Z SPRING SIMULATIONS

Figure 2 shows the idealized soil profile representative of field conditions that is considered in the study of the downdrag problem. The soil profile consists of a clay crust of 2.5 m underlain by a liquefiable layer (LL) of loose sand (D_R = 40%) with a variable thickness of 4 m and 12 m, resting on a dense layer (DL) of sand (D_R = 85%). The water table is located at the ground surface. In this study, three piles representing a large-, medium-, and slender pile are considered. Representative L/D ratios are selected based on commonly used open-pipe piles with length of 18 m

and an outer diameter of 1.45 m, 0.73 m, and 0.36 m, yielding L/D ratios of 12, 15 and 50 respectively. The properties of the piles considered are listed in Table 1.

Both types of end-bearing i.e. floating, and fixed tip are considered. Two post-liquefaction settlement profiles S_1 and S_2 are considered, each one corresponding to reconsolidation strains of 2% in LL and 0% in DL, and 2% in LL and 0.1% in DL respectively. The considered settlement profiles assuming 1-D consolidation, are illustrated in Figure 2.

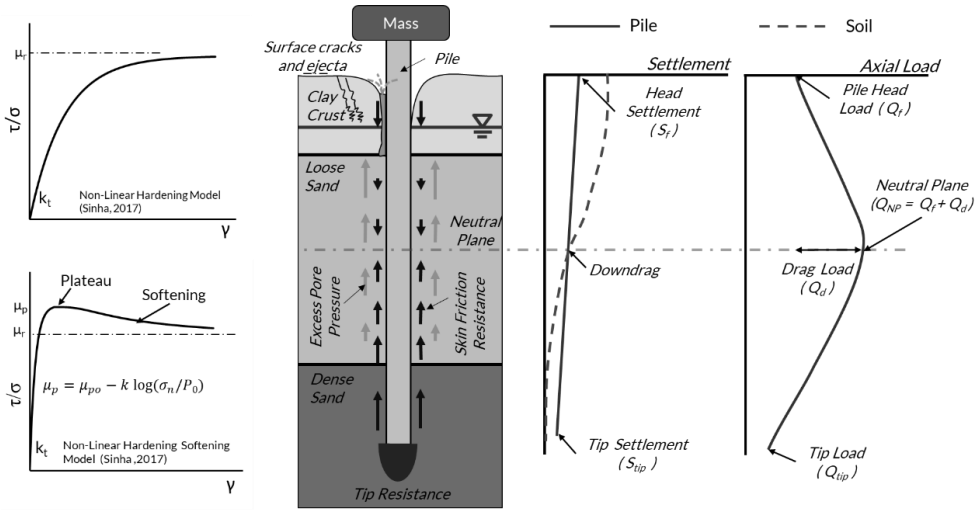

Figure 1. Considered soil-structure interface models and typical settlement and axial load profile for piles in liquefiable soils.

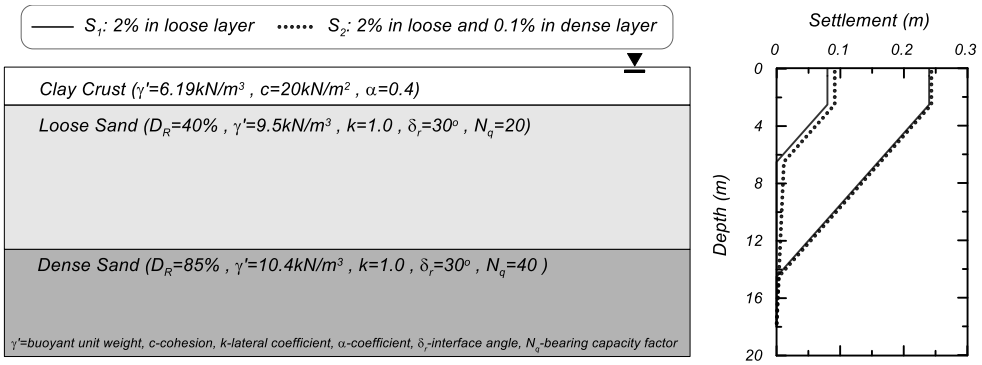

Figure 2. Considered soil profile and reconsolidation settlement.

Table 1. Pile Properties.

Pile Type	Outer Diameter (m)	Thickness (mm)	L/D	Material
Large Pile (LP)	1.45	64	12	Aluminum
Medium Pile (MP)	0.73	34	25	Elastic Modulus: 68 GPa
Slender Pile (SP)	0.36	34	50	Density: 2700 kg/m^3

2.1 *t-z and q-z curves*

The soil-pile interface behavior is modeled using t-z and q-z springs. The interface behavior of clay is modeled using API (2000) recommendations with critical strength factors of 0.8 for large strains. For sands, API (2000) considers a perfectly elastic-plastic curve. However, various researchers (Fakharian 1996; Uesugi & Kishida 1986a, b) have shown that sands can also demonstrate peak and critical shear strength. For this analysis, a critical interface friction angle of δ_r=30^o was considered. The dense sand (D_R=85%) can show a peak behavior (depending upon the confinement level) whereas the loose soil (D_R=40%) is assumed to show only non-linear hardening. The non-linear hardening and non-linear hardening softening model developed by Sinha (2017)

are used in the current analysis to generate the t-z response for the loose and dense sand interfaces respectively (see Fig. 1). These two models have been shown to satisfactorily capture the peak shear strength and stiffness behavior observed in experiments. In the model, the peak normalized shear strength (μ_p) is assumed to degrade with normal stress from the maximum peak normalized shear strength (μ_{po}) to the critical shear strength (μ_r) with a user-defined or calibrated rate of the decrease parameter (k). The shear stiffness (k_t) is taken as 1500 kPa, the softening parameter b = 40, the plateau size parameter n = 8, rate of decrease k = 0.1, and maximum peak normalized friction μ_{po} = 0.8. It should be noted that the shear stiffness (k_t) is increased linearly with normalized normal stress ($\sigma_n/P_{o\ =\ 101.3\ kPa}$). The negative skin friction developed in the reconsolidated liquefied soil is assumed to be equal to the positive non-liquefied value in order to: (a) be more conservative and thus envelope the problem, and (b) facilitate the use of the same interface models to model the interface behavior for both the liquefied and non-liquefied cases. It must also be noted that the analysis presented herein does not consider the effect of pore-pressure generation/dissipation on the interface models.

For the tip, API (2000) recommended q-z curves are used. For the floating tip in the dense sand, a bearing capacity factor of N_q = 40 is assumed, whereas for the fixed tip a large value of N_q = 50,000 is assumed. The maximum displacement required to fully mobilize the tip is taken as 0.1 D (API 2000), where D is the outer diameter of the pile.

2.2 *Analysis and Results*

The analysis is performed in TZPILE (Shin et al. 2018) Version 2014.3.5 with a uniform element size of 0.2 m, and a displacement tolerance of $2x10^{-9}$ m. In the first stage of the analysis, the ultimate total pile capacity ($Q_{total,u}$) and tip capacity ($Q_{tip,u}$) for large, medium and slender piles with floating tip conditions and loose layer thickness of 4 m and 12 m are evaluated. The results are summarized in Table 2. As the pile diameter increases, its total capacity increases due to the increase in the area of the shaft and tip. In the second stage, downdrag analysis is performed with respect to multiple increasing pile head design loads (Q_f) for different pile types, tip conditions, layer thicknesses, and reconsolidation strains. Figures 3-4 illustrate the response for floating and fixed tip cases respectively. The term ($Q_f/Q_{total,u}$) and ($Q_d/Q_{total,u}$) represents the applied pile head load and generated internal drag load (Q_d) normalized with the ultimate pile capacity. The term S_f and S_{tip} represents the settlement of the pile head and the tip respectively. It also plots the settlement as a percentage of the pile diameter (D). Pile compression is the difference between the pile head and the tip settlement.

Table 2. Ultimate resistance of floating piles with bearing capacity factor of (N_q = 40)

Pile Type	Ultimate Total Capacity ($Q_{total,u}$) (kN) LL: 4m	12m	Tip Capacity ($Q_{tip,u}$) (kN)
Large Piles (LP)	14500	12700	11000
Medium Piles (MP)	4300	3400	2750
Slender Piles (SP)	1300	800	700

2.2.1 *Floating Piles*

For no pile head load, the generated drag load is maximized and downdrag is minimized. At this state the neutral plane is at the bottom of the reconsolidating layer and only a small fraction of tip capacity is mobilized. Figure 3 plots the results for floating tip conditions. Increasing the pile head load moves the neutral plane up, correspondingly increasing the downdrag and reducing the drag load (Fig. 3a, b, c). From Figure 3, it can be clearly seen that the drag load decreases with increasing pile head load and ultimately becomes zero at (Q_f / $Q_{total,u}$ = 1). At this state, the neutral plane shifts towards the surface with maximum downdrag and mobilizes the full tip capacity. For all the piles considered, the normalized drag load is higher for the settlement profile S_2 than for S_1, and for each one of them the drag load is greater for thicker liquefiable layers. At the same time, the normalized drag load is greatest for the slender piles.

The rate of decrease in drag load with increasing pile head load is non-linear and depends on the settlement profile and the thickness of the liquefiable layer. For large diameter piles and thinner liquefiable layers with small pile head load, the rate of decrease of drag load is higher for

settlement profile S_2 as compared to S_1 (see Fig. 3a). However, at $Q_f / Q_{total,u}$= 0.4, a sharp transition is observed and the rate of decrease of drag load becomes equal to the one obtained with the settlement profile S_1. This trend is also observed for a liquefiable layer thickness of 8 m but at a much lower normalized pile head load of 0.1. This behavior can be attributed to the fact that, for the settlement profile S_2 with smaller liquefiable layer thickness of 4 m, and smaller pile head load, the neutral plane rests very deep in the dense sand resulting in a higher drag load and a higher rate of decrease with increasing pile head load. However, as the neutral plane moves to the liquefiable layer, the drag load and the rate of its decrease match the ones obtained from the settlement profile S_1, as the soil above the neutral plane contributing to the drag load is the same. The same trend can be seen for other piles. However, the effect is much more prominent for slender piles as the transition zone is achieved at a much higher normalized pile head load.

The settlement at the pile head and tip increases with the increasing pile head load and is higher for thicker liquefiable layers. However, for a small pile head load, the settlements are higher for settlement profile S_2 as compared for profile S_1 (see Fig. 3a, b, c). This behavior is seen more

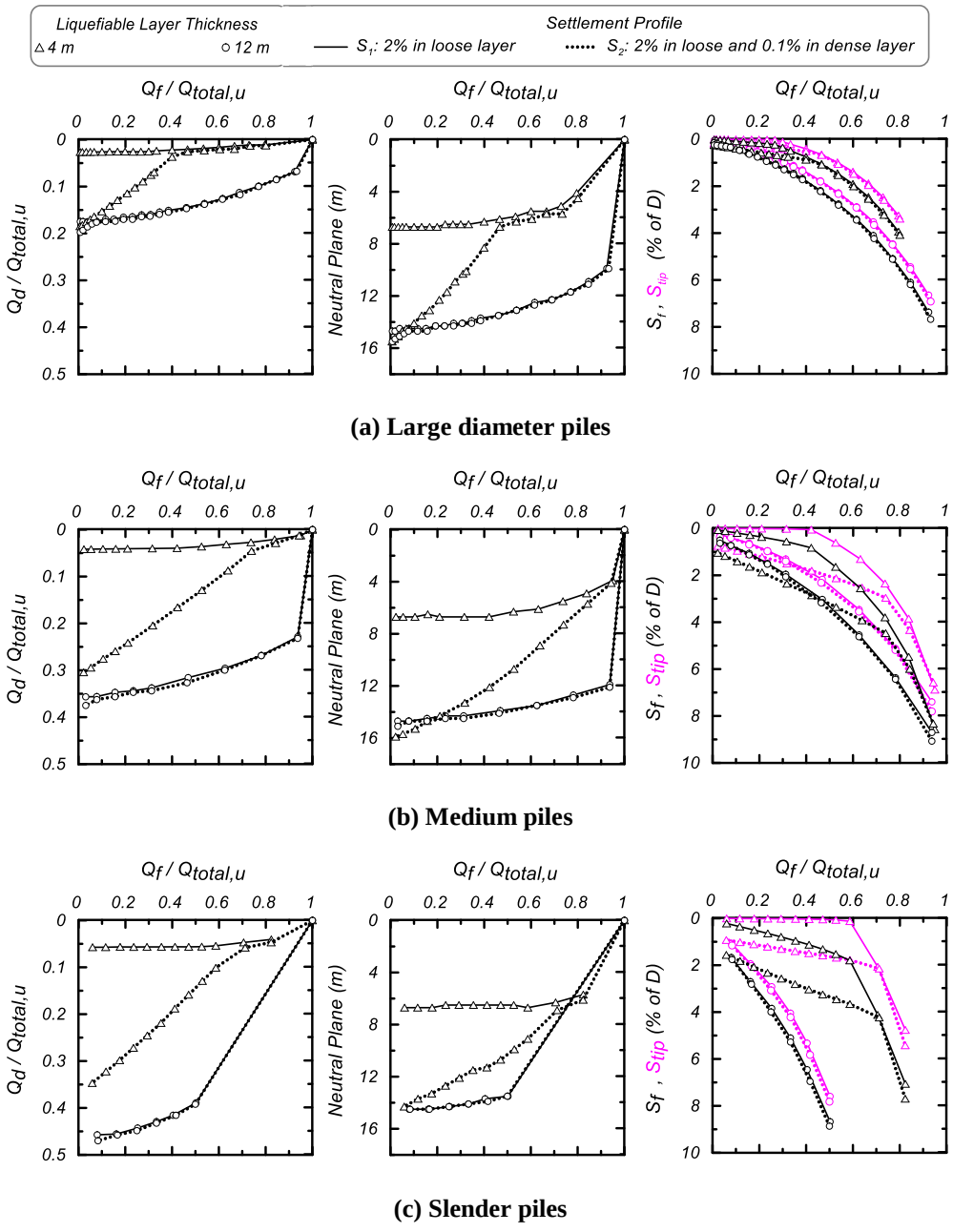

Figure 3. Analysis of (a) LP (b) MP and (c) SP with floating tip condition for varying pile head load.

prominent for the smaller diameter piles (see Fig. 3c). For larger pile head loads, the pile settlements for the two settlement profiles S_1 and S_2 becomes equal. It can also be observed that the slender pile undergoes significantly larger settlements compared to larger diameter pile (Fig. 3c).

The compression observed in the pile is higher for smaller liquefiable layer thickness of 4 m as compared to 12 m and goes maximum up to 2% of D. For a static FOS $\geq$ 1.5 (i.e. Q_f / $Q_{total,u} \leq$ 0.6), the smaller diameter pile not only experiences higher normalized drag load but also are more sensitive to the effects of reconsolidation settlement near tip. Since the tip resistance needs to be mobilized against the generated drag load, it undergoes huge settlements. For large diameter piles, the normalized drag load is less vulnerable to the reconsolidation of dense soil and suffers smaller settlements. It can be seen in Figure 3a, that for (Q_f / $Q_{total,u}$ > 0.4), there is no change in the normalized drag load for settlement profile S_2 as compared to S_1. Medium diameter pile on the other hand, experiences normalized drag load, downdrag and pile settlements between the slender and larger diameter piles.

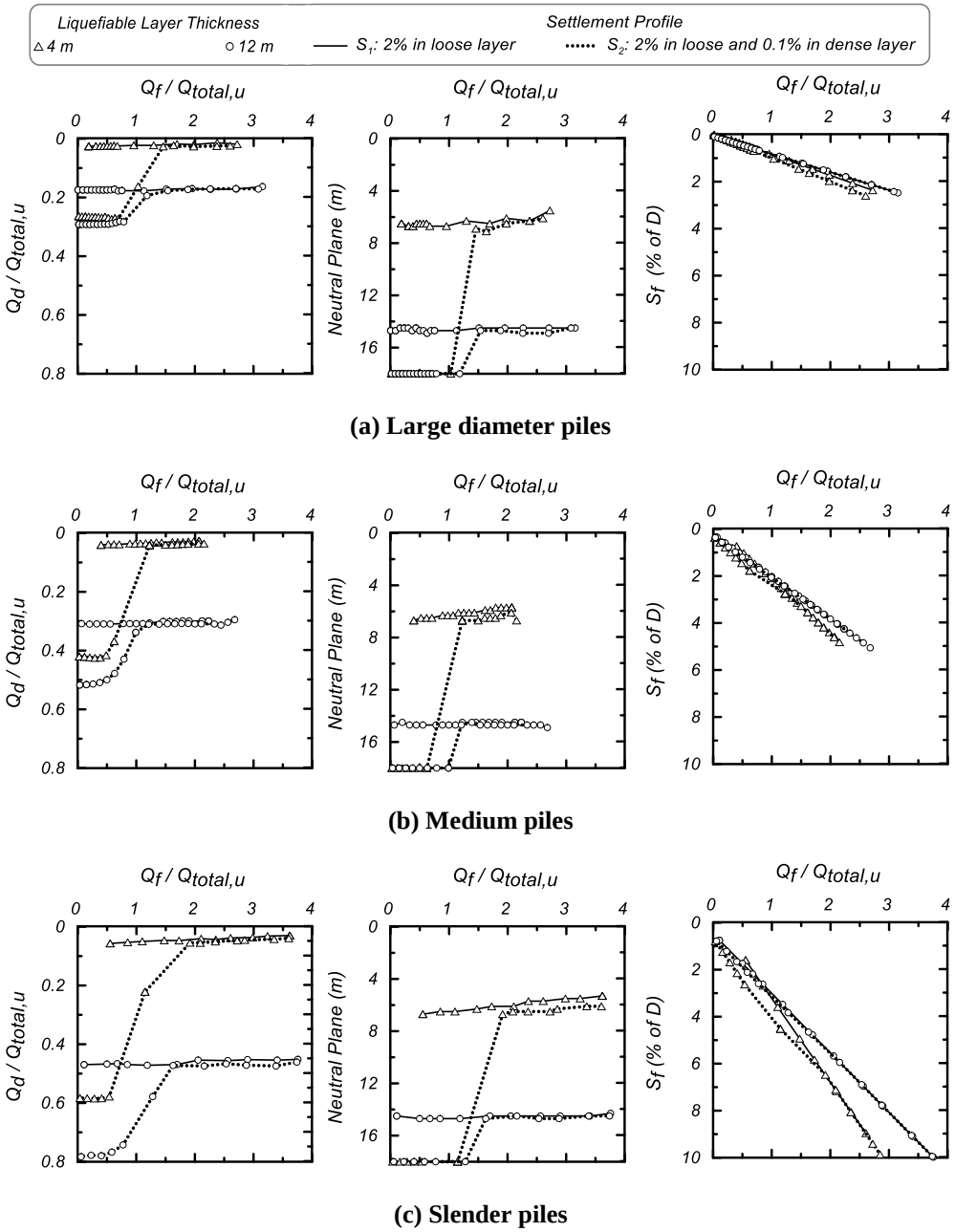

Figure 4. Analysis of (a) LP (b) MP and (c) SP with fixed tip for varying pile head load.

2.2.2 *Fixed Tip Piles*

Fixed tip piles show the same trends as floating piles but experience higher drag loads. In Figure 4, the drag load and the pile head load are normalized with the corresponding ultimate floating pile capacity which results to (Q_f / $Q_{total,u}$) being now greater than 1. Like floating piles, the normalized drag load is higher for the settlement profile S_2 and a transition zone can be seen when the neutral plane shifts from the dense to the loose soil. The normalized drag load, neutral plane, and pile settlements are higher for the settlement profile S_2 which becomes equal to the settlement profile S_1 for a normalized pile head load of about 1.5-2. Because of the tip fixity, the rate of change of location of the neutral plane in the loose soil is very small. Because of the fixed tip, the pile cannot fail in bearing and undergoes huge compression (Fig. 4a, b, c). As a result, serviceability and pile integrity become an important performance criterion. Examining Figure 4 closely, for a smaller pile head load and settlement profile S_2, the generated drag load increases with an increasing pile head load. This effect results from the peak interface behavior of dense sand. With increase in the pile head load, the compression in the pile results in higher relative displacement thus mobilizing the peak shear strength.

Like large diameter floating pile, fixed tip pile is less sensitive to the increasing drag loads due to any reconsolidation settlement of the dense soil near the tip. Assuming that the fixed tip pile is designed with Q_f / $Q_{total,u}$ > 1.5, it can be observed from Figure 4 that its responses does not experience any effect of reconsolidation settlement in the dense soil. The drag load and neutral plane remain almost constant for both profiles S_1 and S_2. However, the pile now experiences huge compression (> 4% of D), which might result in yielding, especially for slender pile (see Fig. 4c).

3 CONCLUSIONS

This paper presented a parametric study performed using the AASHTO-recommended neutral plane method using displacement-based t-z spring analyses. Despite the limitations of the simplified method in not capturing some of the complex mechanisms like excess pore-pressure generations and dissipation in soil, the results obtained draw important conclusions in regard to relative contributions of the liquefied layer thickness, reconsolidation strains in dense soil, and the pile type, on the generated drag load. While a well-calibrated advanced numerical 3-D model would more realistically be able to capture the phenomenon, the conclusions obtained from this study using a method widely used draws important conclusions that still remain useful.

The study shows that as the load at the pile head or design load is increased, the neutral plane shifts up and the drag load reduces. Reconsolidation strains in dense soil near the tip can result in higher drag loads and are more detrimental for smaller diameter piles. For piles with a fixed tip and smaller pile head loads, the settlement of soil near the tip can result in an increase of drag load with increasing pile head load due to the peak interface behavior of dense soil. However, for higher pile head loads, a sharp decline of drag load is observed due to the sudden shift of the neutral plane from the tip to the bottom of the loose soil layer. In floating piles, as the neutral plane shifts from the deeper dense soil with higher interface shear to the shallower loose soil, a transition region of slower decrease of drag load with increasing pile head load is observed.

It is shown that the normalized drag load is higher for the thicker liquefiable layer. For slender piles, it can be as high as 0.5. In general, the normalized drag load is higher for smaller diameter piles than for larger diameter piles for a given normalized pile head load. However, slender piles also undergo huge settlements under the same normalized drag load as compared to larger diameter piles. It is also shown that for a given FOS (~1.5), large diameter piles perform much better (experience smaller normalized drag loads) than smaller diameter piles and are less sensitive to the effects of reconsolidation in the dense sand. On the other hand, piles with fixed tip experience almost 50% higher drag loads than floating piles as well as very high pile compression. Fixed tip piles designed with Q_f / $Q_{total,u}$ > 1.5 do not experience any effect of reconsolidation in dense soil.

The insights gained about the downdrag problem from this study are ultimately used in the design of large centrifuge model tests with the aim of fully understanding the different mechanisms that take place in the field, such as ejecta, surface gaps due to cracking, and excess pore-pressure generation/dissipation patterns which cannot be modelled using existing numerical methods. Since larger diameter piles are less affected by the reconsolidation settlement, testing slender

piles seems to be an obvious choice. However, they can undergo very large settlements or even punching failure even for a lower normalized drag load of 0.6 (see Fig. 3c). On the other hand, for medium piles the normalized drag load and settlement lies in between the slender and large piles. Also, the piles installed in bridges generally represent medium piles. Thus, testing of a medium pile for the centrifuge test is considered. Furthermore, to study the effect of tip resistance, different tip embedments of 0D, 2D, 5D and 8D in dense sand are considered. The prototype steel pipe pile considered has an outer diameter of 0.635 m with a thickness of 11 mm. The L/D ratio depending upon the embedment of the tip will range from 20 to 30. To obtain the correct response of interface behavior and reuse the pile for several tests, axial strain gauges will be installed in the interior wall of the model pile. The experiment will be conducted at the CGM at UC Davis and will be efficiently instrumented to keep track of the development of the drag load, neutral plane, excess pore-pressure generation/dissipation, and the settlement during and post-liquefaction. Results are expected to improve understanding of the different mechanisms affecting the liquefaction induced downdrag and facilitate the development of guidelines for their assessment.

4 ACKNOWLEDGEMENT

This work was funded by the California Department of Transportation under Agreement 65A0688. The authors would like to acknowledge Caltrans engineers and staff involved in this project for the suggestions and assistance, as well as the anonymous reviewer for providing valuable comments on this work.

REFERENCES

AASHTO. 2014. LRFD Bridge Design Specifications. American Association of State Highway and Transportation Officials.

API. 2000. Recommended practice for planning, designing and constructing fixed offshore platforms — Working Stress Design. *API Recommended Practice* 2A–WSD(December 2000).

Ashford, S.A., Rollins K.M. & Lane, J.D. 2004. "Blast-induced liquefaction for full-scale foundation testing." *Journal of Geotechnical and Geoenvironmental Engineering* 130(8): 798–806.

Boulanger, R.W. & Brandenberg, S.J. 2004. Neutral plane solution for liquefaction-induced down-drag on vertical piles. *Geotechnical Engineering For Transportation Projects*: 470–78.

Coelho, P.A.L.F., Haigh, S.K. & Madabhushi, S.P.G. 2004. Centrifuge modelling of earthquake effects in unifrom deposits of saturated sand. *5th International Conference on Case Histories in Geotechnical Engineering, New York, April 13-17* (36).

Fakharian, K. 1996. Three dimensional monotonic and cyclic behaviour of sand-steel interfaces: testing and modeling. Carleton University and University of Ottawa.

Fellenius, B.H. & Siegel, T.C. 2008. Pile drag load and downdrag in a liquefaction event. *Journal of Geotechnical and Geoenvironmental Engineering* 134(9): 1412–16.

Knappett, J.A. & Madabhushi, S.P.G. 2006. Modeling of liquefaction-induced instability in pile groups. *Seismic Performance and Simulation of Pile Foundations*: 255–67.

Rollins, K.M. & Strand, S.R. 2006. Downdrag forces due to liquefaction surrounding a pile. *8th U.S. National Conference on Earthquake Engineering*: 1-10.

Rollins, K.M. & Hollenbaugh, J.E. 2015. Liquefaction induced negative skin friction from blast-induced liquefaction tests with auger-cast piles. *6th International Conference on Earthquake Geotechnical Engineering*: 4–11.

Rollins, K.M., Gerber, T.M., Lane, J.D. & Ashford, S.A. 2005. Lateral resistance of a full-scale pile group in liquefied sand. *Journal of Geotechnical and Geoenvironmental Engineering* 131: 115–25.

Shin, L.C.R., Wang, T. & Arrellaga, J.A. 2018. Analysis of load versus settlement for an axially-loaded deep foundation TZPILE 2014 – User's Manual.

Sinha, S.K. 2017. Modeling of dry and saturated soil-foundation interfaces. University of California Davis.

Uesugi, M. & Kishida, H. 1986a. Frictional resistance at yield between dry and mild steel. *Soils and Foundations* 26(4): 139–49.

Uesugi, M. & Kishida, H. 1986b. Influential factors of friction between steel and dry sands. *Soils and Foundations* 26(2): 33–46